Development 136, 3475-3484 (2009) doi:10.1242/dev.040220

Dendrite branching and self-avoidance are controlled by Turtle, a conserved IgSF protein in *Drosophila*

Hong Long*, Yimiao Ou*, Yong Rao† and Donald J. van Meyel†

The dendritic trees of neurons result from specific patterns of growth and branching, and dendrite branches of the same neuron avoid one another to spread over a particular receptive field. Recognition molecules on the surfaces of dendrites influence these patterning and avoidance processes by promoting attractive, repulsive or adhesive responses to specific cues. The *Drosophila* transmembrane protein Turtle (Tutl) and its orthologs in other species are conserved members of the immunoglobulin superfamily, the in vivo functions of which are unknown. In *Drosophila* sensory neurons, we show that the *tutl* gene is required to restrain dendrite branch formation in neurons with simple arbors, and to promote dendrite self-avoidance in neurons with complex arbors. The cytoplasmic tail of Tutl is dispensable for control of dendrite branching, suggesting that Tutl acts as a ligand or co-receptor for an unidentified recognition molecule to influence the architecture of dendrites and their coverage of receptive territories.

KEY WORDS: Neuron, Dendrite, *Drosophila*, Arborization, Repulsion

INTRODUCTION

Developing neurons form dendritic trees with cell type-specific patterns of arborization, ranging from simple arbors with few branches to highly elaborate arbors that cover receptive territories with many branches. In neurons with even the most complex trees, dendrite branches growing from the same neuron (isoneuronal branches) avoid one another as they spread over a territory to receive sensory or synaptic inputs. Together, dendrite branching and self-avoidance are crucial for sculpting the particular architecture of a neuron's receptive field. Both processes are thought to be controlled by molecular recognition events that occur between isoneuronal branches, or between dendrites and the substrata along which they grow. However, few of the molecules participating in these recognition events have been described.

Cell surface recognition molecules that promote dendrite growth and/or branching include cadherins (Gao et al., 2000; Kimura et al., 2006; Shima et al., 2007; Sweeney et al., 2002), as well as those mediating responses to neurotrophins (Horch and Katz, 2002), B-type ephrins (Horch and Katz, 2002), and cues that direct dendritic guidance, such as Semaphorins (Komiyama et al., 2007; Polleux et al., 2000), Slits (Dimitrova et al., 2008; Furrer et al., 2007; Godenschwege et al., 2002; Whitford et al., 2002) and Netrins (Furrer et al., 2003). In contrast to these examples, which promote or guide dendrite arborization, recognition molecules that prevent inappropriate or excessive dendrite branching in neurons with simple arbors remain unidentified.

Recognition mechanisms underlying dendrite self-avoidance have only recently emerged, with findings that the Dscam family of immunoglobulin superfamily (IgSF) proteins promote self-avoidance in *Drosophila* (Hughes et al., 2007; Matthews et al., 2007; Soba et al., 2007) and mice (Fuerst et al., 2008). It remains to be determined whether other families of cell surface proteins are also required to promote self-avoidance.

The identification of novel transmembrane proteins required for dendrite branching and self-avoidance is a key step in understanding molecular mechanisms that underlie dendrite patterning. The *Drosophila* protein Turtle (Tutl) and its mammalian orthologs, Dasm1 (Igsf9) in mice and IGSF9 (KIAA1355) in humans (Doudney et al., 2002; Shi et al., 2004), are type 1 transmembrane proteins with an ectodomain comprising five immunoglobulin (Ig)-like domains and two fibronectin type III repeats (Fig. 1A). In *Drosophila*, mutations of the *tutl* gene impair responses to tactile stimuli and the execution of complex coordinated behaviors (Bodily et al., 2001), but the causes of these nervous system deficits are unknown. To date, no morphological defects have been reported for *tutl* mutants, despite the structural similarity of Tutl to the Neogenin, Deleted in Colorectal Carcinoma, Frazzled and Roundabout families of axon guidance receptors (Bodily et al., 2001).

In mice, the Tutl ortholog Dasm1 is selectively expressed in the developing hippocampus (Mishra et al., 2008; Shi et al., 2004). Dasm1 knockout mice have no observable defects in dendrite morphogenesis in the developing hippocampus, nor have defects of neuronal differentiation, synaptogenesis or behavior been seen in these mice (Mishra et al., 2008). Therefore, the role Dasm1 in the mammalian nervous system remains uncertain, and genetic approaches to study Dasm1 function in mice could be complicated by redundancy of Dasm1 with Igsf9b, a closely related protein (Mishra et al., 2008).

Here, we have used genetic approaches to study the effects of *tutl* mutations on dendritic arborization (da) neurons in the *Drosophila* peripheral nervous system. We found that Tutl is expressed on dendrites of da neurons and, through loss-of-function and gain-of-function experiments in vivo, we demonstrate that Tutl cell-autonomously controls dendrite branching and self-avoidance. Tutl restricts branching in neurons with simple arbors and promotes self-avoidance in neurons with highly complex arbors. These results demonstrate that a member of the Tutl/Dasm1/IGSF9 family of proteins can influence dendrite morphogenesis in vivo, and that neurons

Centre for Research in Neuroscience and Department of Neurology and Neurosurgery, McGill University, and the McGill University Health Centre Research Institute, Montreal, QC, Canada.

*These authors contributed equally to this work
†Authors for correspondence (yong.rao@mcgill.ca; don.vanmeyel@mcgill.ca)

Accepted 19 August 2009

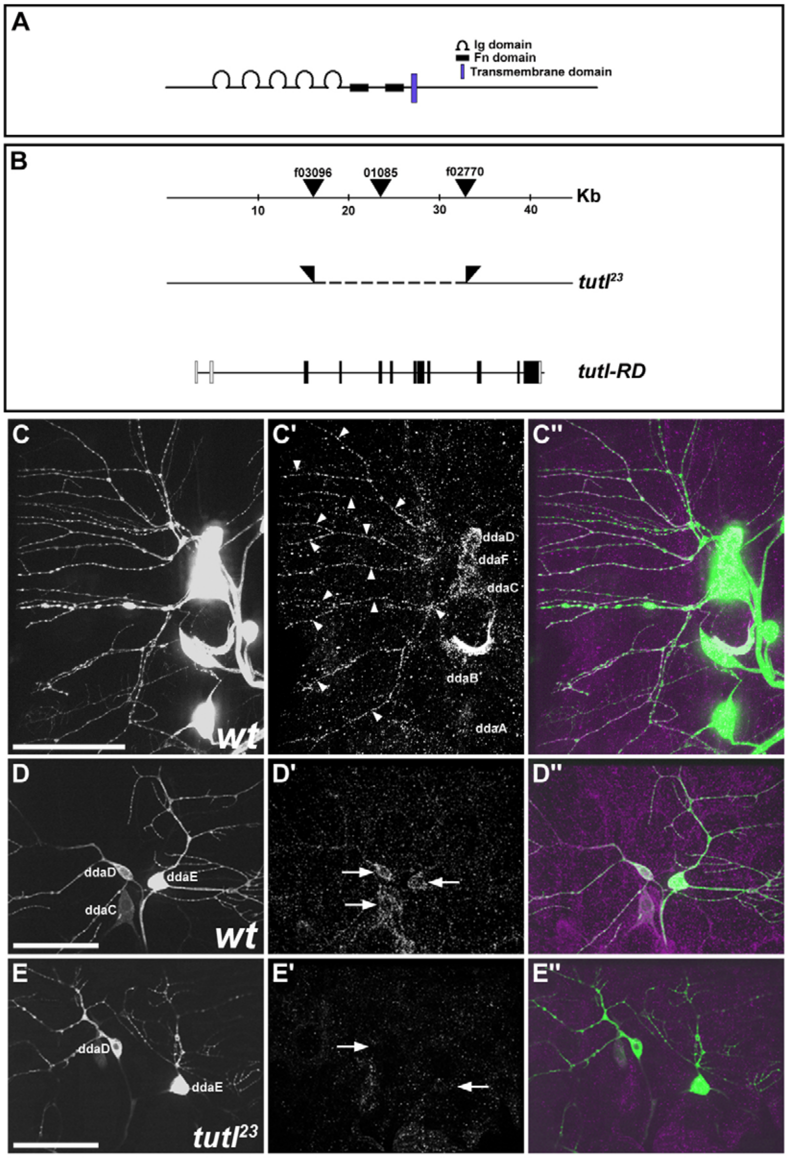

Fig. 1. Tutl protein structure, *tutl* alleles, and Tutl expression in da neurons. (**A**) Schematic diagram of the Tutl protein. (**B**) Structure of the *tutl* locus and position of *tutl* mutations. The P-element causing *tutl*^{01085} is inserted in the fifth exon of *tutl*. The *tutl*^{23} mutation was generated by excising the genomic DNA between the PBac elements f03096 and f02770. *tutl*-RD (FlyBase) encodes full-length *tutl* corresponding to EST RE40452. (**C**) *UAS-mCD8::GFP* driven by *GAL4*$^{109(2)80}$ was used to visualize the cell bodies and dendrites of dorsal da neurons of wild-type third-instar larvae. (**C′**) Tutl immunoreactivity was observed in da neuron cell bodies (labeled) and dendrites (arrowheads). The majority of the dendrites labeled here belong to the class I da neuron ddaD. (**C″**) Overlay of GFP (green) and Tutl (magenta). (**D**) Class I da neurons (ddaD and ddaE) visualized by *GAL4*^{221}-driven expression of mCD8::GFP; there was also weak ectopic expression of GFP in class IV ddaC. (**D′**) Tutl was expressed in the cell bodies of GFP-positive da neurons. (**D″**) Overlay of GFP (green) and Tutl (magenta). (**E-E″**) In *tutl*^{23} homozygous mutants, Tutl staining was absent from GFP-positive da neurons. Scale bars in C-E: 50 μm. Anterior is left, dorsal up.

of different classes employ Tutl as a common molecular component of mechanisms that sculpt dendrite arborization patterns of dramatically different complexity.

MATERIALS AND METHODS

Fly stocks and genetics

Flies were obtained from stock centers at Bloomington [*tutl*^{01085}, *tutl*^{Df} (Df(2L)ed-dp)] and Harvard (*tutl*^{f03096} and *tutl*^{f02770}), and from published sources (*GAL4*$^{109(2)80}$, *GAL4*^{221}, *ppk1.9-GAL4*, *UAS-mCD8::GFP*). We generated *tutl*^{23} by FLP/FRT-mediated recombination (Parks et al., 2004) to delete the intervening DNA between *tutl*^{f03096} and *tutl*^{f02770}, leaving a reconstituted WH PBac element at the deletion site (Fig. 1B), as confirmed by PCR and DNA sequencing. We generated *UAS-tutl* by cloning into the pUAST vector a 5.2-kb *Eco*RI/*Bam*HI fragment from the EST RE40452, which encodes full-length *tutl* corresponding to tutl-RD in FlyBase (Fig. 1B). For *UAS-tutlΔcyto,* we used PCR (oligonucleotide primers: 5′-ACG ACT CAC TAT AGG GCG-3′ and 5′-CGC C<u>TC</u> <u>TAG</u> <u>A</u>CT ATA CGG CAC AAA C-3′) to amplify a fragment from EST RE40452. The second primer introduced a stop codon and an *Xba*I site (underlined). The fragment was cut with *Eco*RI and *Xba*I and introduced into *Eco*RI/*Xba*I-restricted pUAST. *UAS-tutlΔcyto* encodes a truncated Tutl protein comprising Tutl amino acids 1-879 predicted by Tutl-RD.

For *tutl* MARCM, virgin females of the stock *elav*^{C155}*-GAL4,UAS-mCD8::GFP,hs-FLP; FRT40A,tub-GAL80* were crossed to males that were either *elav*^{C155}*-GAL4,UAS-mCD8::GFP,hs-FLP;FRT40A* or *elav*^{C155}*-GAL4,UAS-mCD8::GFP,hs-FLP;FRT40A, tutl*^{23}. For *cut* MARCM, flies of the stock *FRT19A, tub-GAL80, hs-FLP; GAL4*$^{109(2)80}$*, UAS-mCD8::GFP* were crossed to flies carrying *FRT19A*, *cut*^{c145}*/FM7c*. Embryos were collected for 2 hours, incubated at 25°C for 2-3 hours, then heat shocked at 38°C for 1 hour and incubated at 25°C until they were analyzed just prior to pupation. Larvae mutant for *tutl* were cultivated on agar plates. Mutant animals were selected with the aid of balancer chromosomes *CyO,twi-Gal4,UAS-GFP* (for *tutl*, *ab* and *kn*) or *TM3,twi-Gal4,UAS-GFP* (for *ss*).

Imaging and quantification

Larvae were dissected in PBS and GFP-positive da neurons were imaged with confocal microscopy using a Yokogawa spinning disk system (Perkin-Elmer) on an Eclipse TE2000-U microscope (Nikon). *z*-series images were collected using Metamorph software (Molecular Devices) and prepared for publication in Photoshop by converting images to grayscale and adjusting brightness and contrast. Reconstruct software (Fiala, 2005) was used to quantify the numbers of branch termini, branch points and crossing points, as well as dendritic length (classes I-III) and dendritic field area [polygon method (Grueber et al., 2002)]. The dendritic arbors of class IV neurons

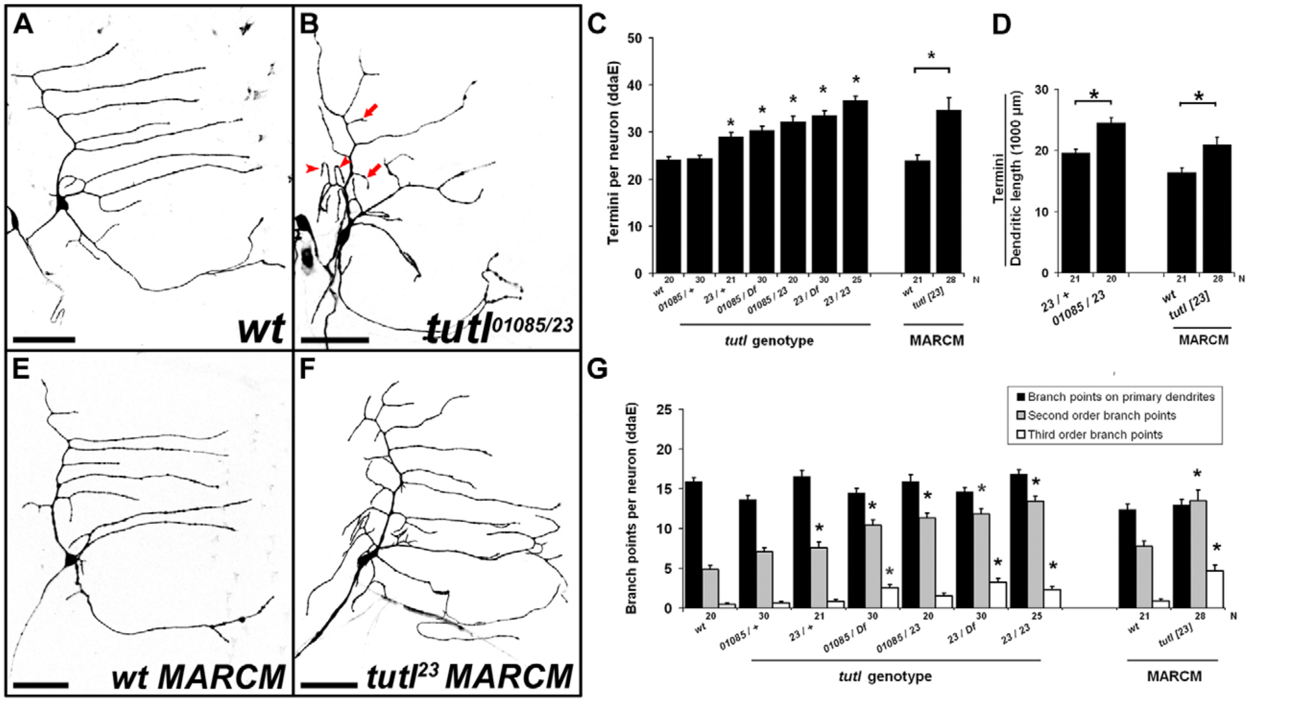

Fig. 2. *tutl* is required to restrain dendrite branching in class I da neurons. (**A**,**B**) Class I ddaE neuron visualized by $GAL4^{221}$ driving *UAS-mCD8::GFP*. (A) ddaE neuron in wild type (wt). (B) ddaE neuron in $tutl^{01085/23}$ mutant with dendrite defects, including shortened interstitial branches (arrows) and curled growth lacking directed orientation (arrowheads). (**C**) Quantification of ddaE branch termini in wild type and *tutl* mutants. Bars show mean±s.e.m. Asterisks indicate significant difference from wild-type (wt) control, ANOVA ($P<1\times10^{-4}$). In similar ANOVA tests, the $tutl^{23/+}$ heterozygotes were also significantly different from $tutl^{23/Df}$ and $tutl^{23/23}$ mutants. (**D**) Normalization of branch termini to dendritic length (mean±s.e.m.; asterisks: *tutl* mutants, *t*-test, $P<4\times10^{-5}$; *tutl* MARCM, *t*-test, $P<0.008$). (**E**,**F**) MARCM clones of ddaE neurons. (E) Wild-type ddaE clone. (F) $tutl^{23}$ clone showing increased numbers of branch termini and branch points compared with wild type. (**G**) Quantification of branch points (asterisks: *tutl* mutants compared to wild-type control, ANOVA, $P<0.01$, except $tutl^{23}$/+ versus wild-type control, ANOVA, $P<0.05$; $tutl^{23}$ MARCM clones versus wild-type clone controls, *t*-test, $P<0.002$). Scale bars in A,B,E,F: 50 µm. Anterior is left, dorsal up. N, number of neurons quantified for each genotype. Genotypes: A, $GAL4^{221}$,*UAS-mCD8::GFP*/+; B, $tutl^{01085}$/$tutl^{23}$;$GAL4^{221}$,*UAS-mCD8::GFP*/+; E, $elav^{C155}$-*GAL4,UAS-mCD8::GFP,hs-FLP;FRT40A*; F, $elav^{C155}$-*GAL4,UAS-mCD8::GFP,hs-FLP;FRT40A,*$tutl^{23}$.

were traced and measured with Imaris software (Bitplane). The data were tested for normal distribution using the Shapiro-Wilk test, and statistical analysis was performed using Analyse-It software for Microsoft Excel.

Immunohistochemistry

Anti-Tutl polyclonal antiserum was raised in rabbits to a GST-Tutl (amino acids 1-421) fusion protein corresponding to immunoglobulin (Ig) domains 1-3 of the Tutl ectodomain, then affinity-purified and pre-absorbed using standard methods. For anti-Tutl immunofluorescence, embryos or third instar larvae were dissected in PBS and fixed in 4% paraformaldehyde (Ou et al., 2008), then anti-Tutl antibody (1:25, 4°C) was detected with Rhodamine Red-X-conjugated secondary antibody (1:300). In double labeling of embryos for Tutl and HRP, we also added Cy2-conjugated anti-HRP (1:500, 4°C). Prior to mounting samples from third instar larvae, muscles overlying the dorsal cluster da neurons were removed by dissection for better visualization.

RESULTS

Tutl expression in da neurons

Four da neuron classes (I-IV) of increasing dendritic complexity and size can be readily observed in the larval body wall of *Drosophila*, sandwiched in two dimensions between muscles and epidermis (Grueber et al., 2002). We focused on the dorsal-most cluster of peripheral sensory neurons, which contains at least one representative from each class. We examined Tutl expression with immunofluorescence and found that Tutl was expressed in the cell bodies and along the dendrites of class I neurons ddaD and ddaE in third instar larvae (Fig. 1C′,D′). Class I neurons have the least complex arbors of all da neurons. Tutl was also readily observed in the cell body of the class IV neuron ddaC (Fig. 1C′,D′), the arbors of which are the most complex. Tutl was also expressed in the class II neuron ddaB and the class III neurons ddaA and ddaF (Fig. 1C′), in addition to in other sensory neurons in the dorsal cluster (see Fig. S4 in the supplementary material). The specificity of the antibody for Tutl was confirmed by the absence of expression in $tutl^{23}$ mutants (Fig. 1E′), which carry a novel *tutl* allele (Fig. 1B).

Analysis of Tutl function in class I da neurons

To examine the phenotypical consequences of *tutl* mutations in da neurons, we studied $tutl^{23}$ and other available P-element insertion ($tutl^{01085}$) and deficiency ($tutl^{Df}$) alleles. We began by examining dendrite morphology of the class I da neuron ddaE, using the class I driver $GAL4^{221}$ and *UAS-mCD8::GFP* as a reporter to reveal the dendritic tree (Grueber et al., 2003). In control larvae at third instar, ddaE neurons have a simple, comb-like appearance (Fig. 2A) and 24.1±0.8 (mean±s.e.m.) branch termini per cell (Fig. 2C). One of the two or three primary dendrites projects dorsally and gives rise to several lengthy interstitial secondary branches that grow in a posterior direction toward the segment boundary (Fig. 2A). By contrast, the dendritic trees of ddaE neurons in homozygous or hetero-allelic *tutl* mutants had a number of defects, including

DEVELOPMENT

severely shortened interstitial branches and irregular patterns of curled or tortuous growth, which often lacked directed orientation (Fig. 2B; see Fig. S1A-C in the supplementary material). We scored these defects while blind to genotype, and found them in 20/20 ddaE neurons from *tutl*^{01085}/*tutl*^{23} mutants, but in only 2/20 wild-type controls, which indicated a high penetrance of the *tutl* mutant phenotype. In addition, compared with wild-type ddaE neurons, we found significantly more branch termini (Fig. 2B; Fig. S1A-C in the supplementary material), increasing to 36.7±0.9 in *tutl*^{23} homozygotes (Fig. 2C). This was as severe as in *tutl*^{23}/*tutl*^{Df} hemizygotes (33.5±1.1; Fig. 2C; Fig. S1B in the supplementary material), supporting our molecular and immunochemical data that *tutl*^{23} is a null allele of *tutl*. Heterozygotes (*tutl*^{23}/+) had a degree of branching that was intermediate between controls and homozygotes (Fig. 2C), suggesting that ddaE branching is sensitive to the levels of Tutl. Overall, the mutant genotypes had increases in ddaE branches that ranged from 126-152% of wild-type controls (Fig. 2C). Similar observations were made for ddaD (not shown), another class I da neuron.

Single-cell analysis of Tutl function in da neuron dendrite branching

Although Tutl is expressed in dendrites of class I da neurons, the phenotypes we observed could result from either cell autonomous or non-cell autonomous Tutl activity. To investigate whether *tutl* is required cell autonomously in class I da neurons, we generated single mutant neuron clones using the MARCM system (Lee and Luo, 1999). Control ddaE MARCM clones exhibited normal morphology and branching (24.0±1.2; Fig. 2C,E), but the dendrites of *tutl*^{23} ddaE MARCM clones showed increased branch termini to the same level as that found in *tutl* mutant animals (34.7±2.6; Fig. 2C,F). Other features of the *tutl* homozygous mutant phenotype (i.e. shortened interstitial branches, irregular patterns and directions of growth) were not readily observed in *tutl*^{23} ddaE MARCM clones, and thus we are unable to ascribe them to cell autonomous loss-of-Tutl function. Therefore, we focused on the role of Tutl in the control of dendrite branching, where MARCM analysis pointed to a specific and cell autonomous role for Tutl in preventing excessive dendrite branching.

When normalized for dendritic length, ddaE neurons in *tutl*^{01085}/*tutl*^{23} mutants and *tutl*^{23} MARCM clones retained increased numbers of branch termini relative to controls (Fig. 2D; see also Fig. S2A in the supplementary material), which suggests that *tutl* mutations increase dendrite branching complexity independently of ddaE dendrite growth. We analyzed the branching defect of *tutl* mutants in more detail by counting (1) branch points on primary dendrites that project directly from the cell body, and (2) second or third order branch points situated more distally on the arbor (Fig. 2G). Although the number of branch points on primary dendrites was unchanged in *tutl* mutants and *tutl*^{23} MARCM clones, there was a clear increase in the number of second and third order branch points.

To determine whether Tutl cell autonomously inhibits branching in other classes of da neurons, we used MARCM to examine class II (ddaB), class III (ddaA, ddaF) and class IV (ddaC) neurons (Grueber et al., 2002). In *tutl*^{23} MARCM clones for neurons of class II (Fig. 3A-D) and class III (Fig. 3E-H), we found no significant changes of branch number nor did we observe any effects on the pattern, growth or targeting of their dendritic trees. In the class IV neuron ddaC, we observed defects in dendrite self-avoidance (see below), but branch number was unaffected (see Fig. S2B in the supplementary material, MARCM data). Together, these results indicate that *tutl* has class-specific effects on dendrite branching in vivo.

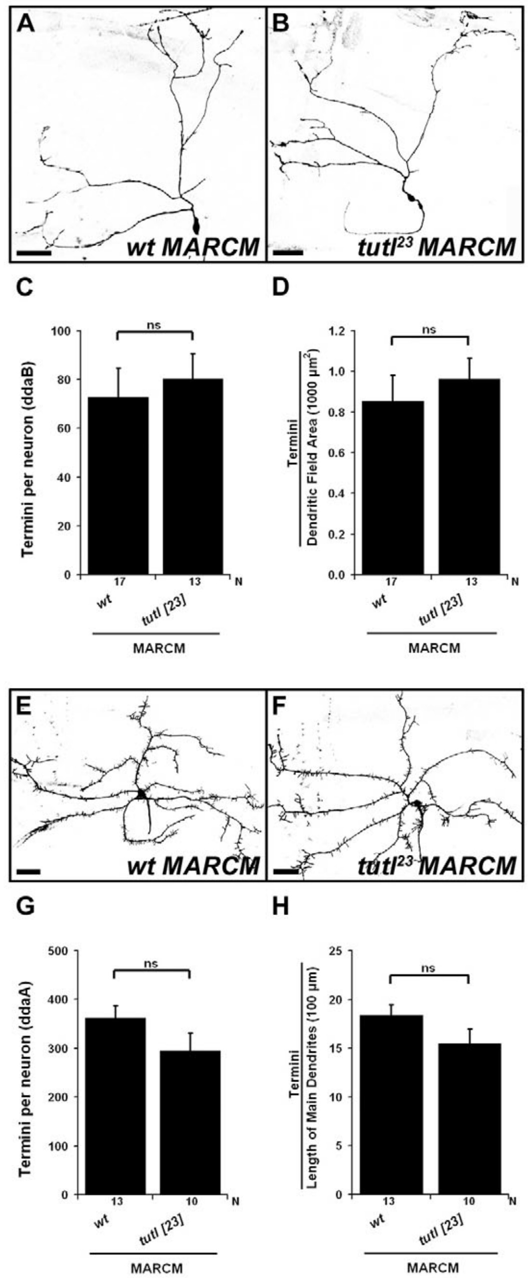

Fig. 3. Class II and class III da neurons are unaffected in *tutl*^{23} MARCM clones. (**A**,**B**) MARCM clones of class II ddaB neurons. (A) Wild-type ddaB clone. (B) *tutl*^{23} mutant ddaB clone showing normal dendritic pattern. (**C**) Quantification of ddaB termini (mean±s.e.m.), showing no significant (ns) difference between wild-type and *tutl*^{23} MARCM clones (*t*-test, $P>0.05$). (**D**) Quantification of ddaB termini normalized to dendritic field area (mean±s.e.m.), again showing no significant difference. (**E**,**F**) MARCM clones of class III ddaA neurons. (E) Wild-type clone; (F) *tutl*^{23} MARCM ddaA clone. (**G**) Quantification of ddaA termini (mean±s.e.m.). (**H**) Quantification of ddaA termini normalized to the total length of the main dendritic branches of ddaA (mean±s.e.m.), not including spine-like protrusions.

Effects of *tutl* mutation on class IV da neurons

Dendrite self-avoidance involves repulsive interactions between isoneuronal branches following transient contact (Hughes et al., 2007; Matthews et al., 2007; Soba et al., 2007). To investigate the role of *tutl* in dendrite self-avoidance, we examined the complex

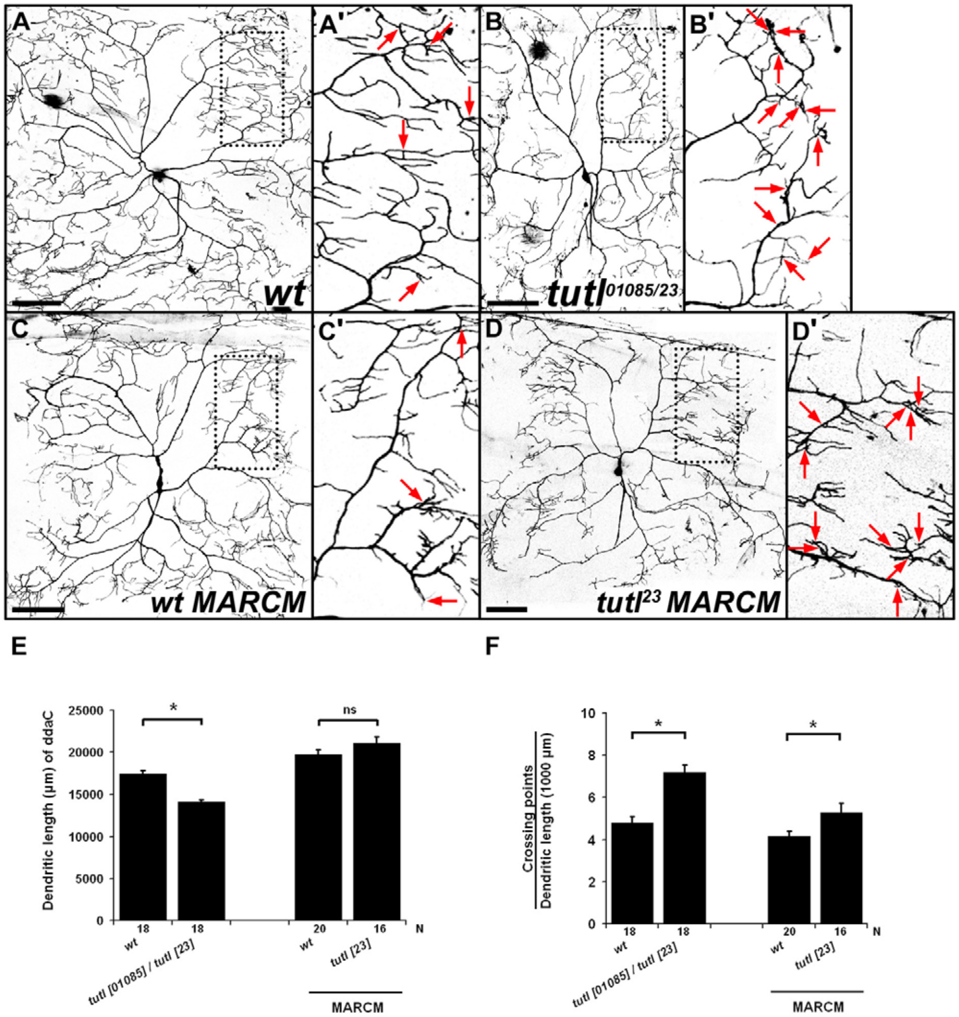

Fig. 4. *tutl* is required for dendrite self-avoidance in class IV da neurons. (**A-B′**) Class IV ddaC neurons visualized by *ppk1.9-GAL4* driving *UAS-mCD8::GFP*. (A) ddaC neuron in wild type. Dotted outline marks area shown in A′. (A′) Branches of ddaC neurons normally show self-avoidance, with only occasional crossing points (arrows). (B,B′) ddaC neuron in $tutl^{01085/23}$ mutant showed numerous dendrite crossing points (arrows). The dendritic field is smaller than that of wild type because *tutl* mutant animals are shorter than wild type. (**C-D′**) MARCM clones of ddaC neurons. (C,C′) Wild-type ddaC clone showed self-avoidance and occasional crossing points (arrows). (D,D′) $tutl^{23}$ clone showed increased numbers of crossing points (arrows). (**E**) Quantification of dendrite length in ddaC neurons (mean±s.e.m.; asterisks: *tutl* mutants, *t*-test, $P<3\times10^{-7}$; *tutl* MARCM, *t*-test, P=0.144; ns, not significant; N, number of neurons quantified for each genotype). (**F**) Quantification of dendrite crossing points normalized to dendritic length in ddaC neurons (mean±s.e.m.; *tutl* mutants, *t*-test, $P<2\times10^{-5}$; *tutl* MARCM, *t*-test, $P<0.03$). Scale bars in A,B,C,D: 100 μm. Anterior is left, dorsal up. Genotypes: A,A′, *UAS-mCD8::GFP/+;ppk1.9-GAL4/+*; B,B′, *UAS-mCD8::GFP/+;*$tutl^{01085}/tutl^{23}$*;ppk1.9-GAL4/+*; C,C′, $elav^{C155}$*-GAL4,UAS-mCD8::GFP,hs-FLP*; *FRT40A*; D,D′, $elav^{C155}$*-GAL4, UAS-mCD8::GFP, hs-FLP; FRT40A*, $tutl^{23}$.

arbor of the class IV da neuron ddaC in *tutl* mutants and $tutl^{23}$ MARCM clones. In control third instar larvae, the high-order branches of ddaC seldom overlap with one another (Fig. 4A′,C′). However, in *tutl* mutants (Fig. 4B′) and $tutl^{23}$ MARCM clones (Fig. 4D′), there were increased numbers of crossing points between isoneuronal dendrites. This was not due to any increases in the total length of dendrites (Fig. 4E), nor was it due to any increases in number of branch termini or changes in the area of the dendritic field (see Fig. S2B,C in the supplementary material). In fact, when the number of crossing points was normalized to total dendritic length (Fig. 4E), *tutl* mutants and $tutl^{23}$ MARCM clones showed significant increases in isoneuronal self-crossing to 150% and 127%, respectively, of controls (Fig. 4F). The milder effect using the MARCM technique may be due to the persistence in ddaC clones of residual Tutl protein from precursor cells. The phenotypes induced in *tutl* mutants and *tutl* MARCM clones indicate that Tutl functions within class IV da neurons to prevent overlap between isoneuronal dendrites.

Class IV neurons also exhibit dendritic ‘tiling’, which is the complete and non-redundant coverage of receptive fields by neurons of a similar functional type (Grueber et al., 2002; Parrish et al., 2007). Class IV neurons show tiling with other class IV neurons, even though they overlap extensively with dendrites of class I-III neurons. Like self-avoidance, tiling is thought to be caused by mutual repulsion between dendrites (Parrish et al., 2007), and the processes are related through a common requirement for the nuclear Dbf2-related (NDR) protein kinase Tricornered (Trc) and its putative adaptor protein Furry (Emoto et al., 2004). To determine whether *tutl* is required for dendritic tiling between class IV neurons, we examined the borders between ddaC and another neighboring

DEVELOPMENT

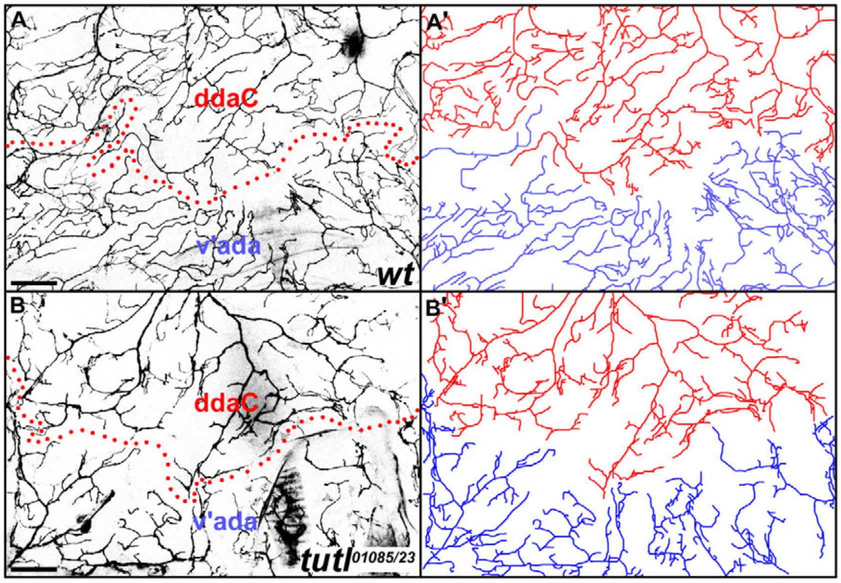

Fig. 5. *tutl* mutants exhibit normal dendritic tiling among class IV da neurons. (**A-B′**) Tiling between class IV da neurons ddaC and v′ada labeled with *ppk1.9-GAL4, UAS-mCD8::GFP*. In A′ and B′, ddaC neurons are traced in red and adjacent v′ada neurons are traced in blue. (A,A′) Class IV neurons in controls established normal territories. (B,B′) Class IV neurons in *tutl* mutants showed intact tiling, but showed defects of self-avoidance. Scale bars in A,B: 50 μm. Anterior is left, dorsal up. Genotypes: A,A′, *UAS-mCD8::GFP/+;ppk1.9-GAL4/+*; B,B′, *UAS-mCD8::GFP/+;tutl^{01085}/tutl^{23}; ppk1.9-GAL4/+*.

class IV neuron (v'ada) for dendritic overlap (Fig. 5A,A′). We found no evidence that *tutl* is required for tiling, as the branches between these different class IV neurons approached one another but did not overlap in *tutl* mutants (Fig. 5B,B′).

Effects of *tutl* overexpression in da neurons

To test whether *tutl* is sufficient to inhibit dendrite branching, we overexpressed full-length Tutl in da neurons using a *UAS-tutl* transgene. In class I neurons (ddaE), branching was unaffected (not shown), suggesting that neurons with small simple arbors and substantial levels of endogenous Tutl along their dendrites are unaffected by adding more Tutl. We then tested the effects of *UAS-tutl* on the large and highly complex dendritic arbors of the class IV da neuron ddaC (Fig. 6A). In contrast to class I ddaE neurons, overexpression of Tutl in ddaC neurons inhibited dendrite branching (Fig. 6B,C).

One idea consistent with the branching and self-avoidance defects caused by *tutl* mutations is that Tutl could promote repulsion between isoneuronal dendrite branches. Repulsion could conceivably induce branch collapse in class I da neurons, or could steer dendrites away from one another in class IV da neurons. To explore whether Tutl is sufficient to repel dendrites away from one another, we exploited the fact that the dendrites of neurons of different classes overlap with one another in the body wall. We used the driver *C161-GAL4* to overexpress *UAS-tutl* in class I, class II and class III neurons simultaneously, but we found no evidence for Tutl-induced repulsion among dendrites of different classes (see Fig. S3 in the supplementary material).

Studies of genetic interactions between *tutl* and mutations of *trc* or *Dscam*

Mutations in *trc* cause excessive branching of class I ddaE neuron dendrites (Soba et al., 2007) and defects of dendrite self-avoidance, particularly at distal branches of the complex arbors of class IV neurons (Emoto et al., 2004). Because mutations of *trc* and *tutl* display these similar features, it is possible that they could act in a common molecular pathway to govern the processes of branch inhibition (class I) and self-avoidance (class IV). We looked for genetic interactions in animals doubly heterozygous for the null mutations *trc^{1}* and *tutl^{23}*, but there were no enhanced branching (class I) or self-avoidance (class IV) defects compared with controls heterozygous for *tutl^{23}* alone (see Table S1 in the supplementary material).

In *tutl* mutants, many isoneuronal dendritic branches still avoid one another appropriately (Fig. 4B,D), suggesting that Tutl is part of a multi-component system that ensures the proper distribution of dendrites over receptive territories. One component of this self-avoidance system involves the diverse family of receptors encoded by the *Dscam* gene. *Dscam* mutants show defects of self-avoidance in all four da neuron classes (Hughes et al., 2007; Matthews et al., 2007; Soba et al., 2007). We examined self-avoidance in class IV neurons, where both genes are required, but found no evidence for genetic interactions between *tutl^{23}* and *Dscam^{33}*, a strong mutant allele of *Dscam* (Hummel et al., 2003) (data not shown).

Investigation of Tutl regulation by transcription factors

Class-specific patterns of da neuron dendrite morphogenesis are regulated by key transcription factors. For example, mutations of the genes encoding the transcription factors Abrupt (Ab) or Spineless (Ss) cause ectopic branching in class I neurons (Kim et al., 2006; Li et al., 2004; Sugimura et al., 2004), resembling the effects we have found for *tutl* mutants. To test whether Tutl expression in class I neurons is regulated by Ab or Ss, we examined Tutl expression in *ab^{k02807}* or *ss$^{D115.7}$* mutants with immunochemistry. Both of these mutant alleles are known to cause defects in dendrite morphogenesis, yet we found no obvious changes in Tutl immunoreactivity (see Fig. S4A-B″ in the supplementary material). Overexpression of Tutl in class IV neurons inhibits dendrite branching, as do mutations in genes encoding the transcription factors Knot (also known as Collier) (Crozatier and Vincent, 2008; Hattori et al., 2007; Jinushi-Nakao et al., 2007) and Cut (Grueber et al., 2003). To explore the possibility that Tutl expression is normally suppressed to endogenous levels in class IV da neurons by Knot or Cut, we examined Tutl protein expression in ddaC neurons in *kn^{KN2}* mutants and *cut^{c145}* MARCM clones. Changes of Tutl immunoreactivity were not detected in da neurons in either case (see Fig. S4C-D″ in the supplementary material).

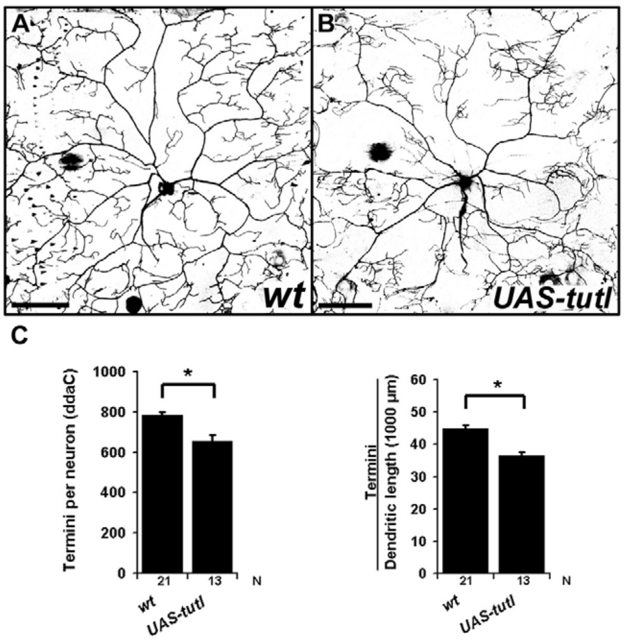

Fig. 6. Overexpression of Tutl inhibits dendrite branching in class IV da neurons. (**A**) Class IV neuron ddaC in wild type. (**B**) Overexpression of Tutl in ddaC reduces branching. (**C**) Quantification of ddaC branch termini per cell, and normalized to dendritic length (asterisks: termini per neuron, *t*-test, $P<2\times10^{-4}$; termini/dendritic length, *t*-test, $P<1\times10^{-5}$). Scale bars in A,B: 100 µm. Anterior is left, dorsal up. N, number of neurons quantified for each genotype. Genotypes: A, *UAS-mCD8::GFP/+;ppk1.9-GAL4/+*; B, *UAS-mCD8::GFP/+; ppk1.9-GAL4/UAS-tutl.*

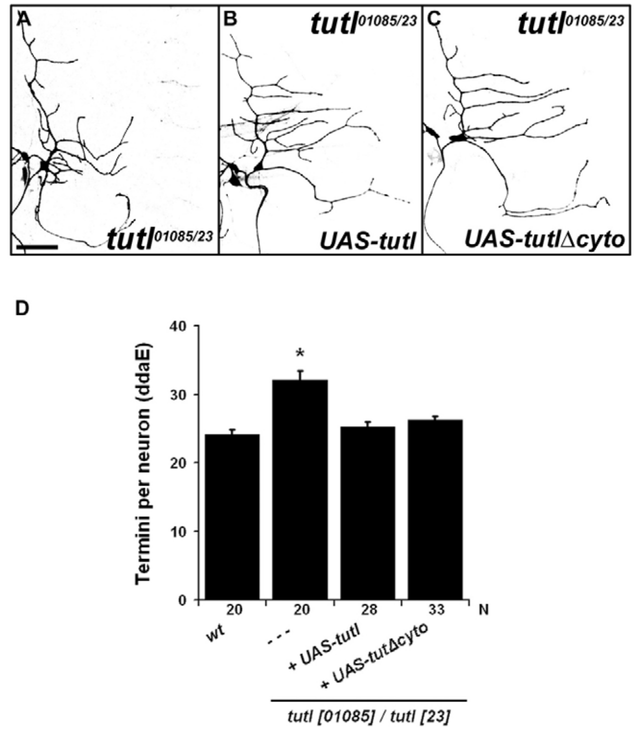

Fig. 7. The cytoplasmic tail of Tutl is dispensable for function in class I da neurons. (**A**) Class I ddaE neuron in $tutl^{01085/23}$ mutant with branching and morphology defects. (**B**) ddaE neuron in $tutl^{01085/23}$ mutant expressing full-length Tutl with $GAL4^{221}$. (**C**) ddaE neuron in $tutl^{01085/23}$ mutant expressing TutlΔcyto. Anti-Tutl immunohistochemistry demonstrating expression of Tutl and TutlΔcyto can be found in Fig. S4 in the supplementary material. (**D**) Quantification of ddaE branch termini in wild type, *tutl* mutants, and rescued animals (mean±s.e.m.). Asterisk indicates significant difference from wild-type (wt) control, ANOVA, $P<1\times10^{-4}$. N, number of neurons quantified for each genotype. Full-length Tutl and TutlΔcyto each rescue the number of branch termini in *tutl* mutants to wild-type levels. Scale bar in A,B,C: 50 µm. Anterior is left, dorsal up. Genotypes: A, $tutl^{01085}/tutl^{23}$;$GAL4^{221}$,*UAS-mCD8::GFP/+*; B, $tutl^{01085}/tutl^{23}$, *UAS-tutl*;$GAL4^{221}$,*UAS-mCD8::GFP/UAS-tutl*; C, $tutl^{01085}/tutl^{23}$;$GAL4^{221}$,*UAS-mCD8::GFP/UAS-tutlΔcyto,UAS-tutlΔcyto*.

Rescue of *tutl* mutant phenotypes and assessment of the dispensability of the Tutl cytoplasmic tail

Tutl and its mammalian orthologs have a conserved ectodomain comprising five Ig-like and two FnIII domains. They also have lengthy but divergent cytoplasmic tails. To begin to investigate the molecular basis for Tutl function in vivo, we wondered whether the cytoplasmic tail of Tutl was dispensable for its function in dendrite morphogenesis. Testing this in class IV da neuron self-avoidance is complicated by the gain-of-function effect of Tutl in ddaC (i.e. branch inhibition). Instead, we examined class I da neurons where Tutl has no gain-of-function effect. We assessed the requirement for the cytoplasmic tail in a rescue assay for branch inhibition in the class I neuron ddaE. To do this, we used $GAL4^{221}$ to specifically express either full-length Tutl or a truncated form lacking the cytoplasmic tail (TutlΔcyto) in class I neurons of *tutl* mutants (Fig. 7; see also Fig. S5 in the supplementary material). The full-length form of Tutl fully restored the number of branch termini per cell (ddaE) to wild-type levels (Fig. 7B,D), providing further confirmation that the phenotype observed in *tutl* mutants was specifically due to the loss of Tutl. Importantly, we found that TutlΔcyto was equally capable of rescuing *tutl* mutants (Fig. 7C,D), which indicates that the cytoplasmic tail of Tutl is indeed dispensable for dendrite branch inhibition in class I da neurons.

Hypomorphic mutants of *tutl* have behavioral defects (Bodily et al., 2001), but strong alleles are lethal. Because Tutl is expressed broadly in the nervous system (Bodily et al., 2001), we used the neural-specific driver $elav^{C155}$-Gal4 to test whether full-length Tutl could rescue viability in $tutl^{23}/tutl^{1085}$ mutants, and whether the cytoplasmic tail was also dispensable for viability. Rescue with full-length Tutl was nearly complete, as 53 of an expected 57 (93%) mutants were rendered viable. The rescued larvae showed normal behavioral responses to tactile stimuli, and could right themselves when overturned (data not shown). By contrast, the rescue with TutlΔcyto was only partial, with 30 viable adults of an expected 152 (20%). Similar results for both full-length Tutl and TutlΔcyto were observed for other *tutl* mutant genotypes, including $tutl^{23}$ homozygotes (data not shown). Together, the data indicate that although the cytoplasmic tail is dispensable for the role of Tutl in limiting dendrite branching in da neurons, it is required for Tutl function in other cell types within the nervous system.

DISCUSSION

Dendrite branching and self-avoidance are two important cellular mechanisms that shape the receptive fields of neurons during development. Here, we have investigated the role of Tutl in these processes using the da sensory neurons of *Drosophila*, an excellent system in which to study dendrite arborization at a single cell level in vivo. Tutl is a member of the

Tutl/Dasm1/IGSF9 family of evolutionarily conserved transmembrane proteins. We have found that Tutl inhibits excessive branch formation in neurons with simple dendrites (class I), and contributes to the processes that prevent crossing of isoneuronal dendrite branches in neurons with complex arbors (class IV), which demonstrates that Tutl influences the architecture of dendrites and their coverage of receptive territories. In contrast to our results for class I and class IV neurons, our MARCM studies found no evidence of a cell-autonomous role for Tutl in class II or class III neurons, despite detectable Tutl expression in their cell bodies. The reasons for a lack of apparent effects on class II or class III da neuron dendrites in *tutl* MARCM clones remain unclear. Sufficient Tutl protein, inherited from precursors, could have remained in MARCM clones to promote normal outgrowth. Alternatively, there might be no role for Tutl in these cells. Nevertheless, it is clear from our results for class I and class IV da neurons that Tutl is required for the arborization of dendritic trees with dramatically different complexity.

A role for Tutl in dendrite branching

Tutl cell-autonomously inhibits dendrite branching in vivo, providing a means by which da neurons with the simplest architecture suppress the formation or stabilization of supernumerary dendrite branches during development. We observed a clear increase in the number of second and third order branch points on *tutl* mutant ddaE neurons. This finding suggests that *tutl* regulates branching only at certain locations along the growing arbor, perhaps by inhibiting branch additions or promoting branch retractions.

The *tutl* phenotype is distinct from that of mutants of *Neuroglian* (*Nrg*), which also encodes a cell surface IgSF protein that affects dendrite branching. Loss of Nrg reduces the number of branches on the dendritic arbors of class I da neurons, and increases branching along their axons, suggesting a role for Nrg in correctly distributing neurites but not as a branching inhibitor (Yamamoto et al., 2006). The *tutl* mutant phenotype is also distinct from the dendrite overgrowth phenotype observed in mutants of the IgSF receptor Robo (Dimitrova et al., 2008), or of the cadherin Flamingo (also known as starry night) (Gao et al., 2000; Kimura et al., 2006; Sweeney et al., 2002). In vertebrate systems, no recognition molecules have yet been shown to inhibit dendrite branching in vivo. However, it is noteworthy that inhibition of axon branching has been demonstrated in the chick visual system, where inappropriate arborization of retinal ganglion cell (RGC) axon terminals is thought to be inhibited by EphA (Yates et al., 2001) and Ryk (Schmitt et al., 2006) receptors. In zebrafish, RGC axons are inhibited from branching by Robo2 (Campbell et al., 2007), an IgSF protein with which Tutl shares homology.

A role for Tutl in dendrite self-avoidance

After Dscam, Tutl is the only cell surface protein that has been shown to be required for dendrite self-avoidance in either invertebrates or vertebrates. As in *Dscam* mutants, the dendrites of *tutl* mutant neurons cross one another with increased frequency, leading to uneven coverage of the receptive field. Unlike Dscam, which promotes self-avoidance in all four da neuron classes (Hughes et al., 2007; Matthews et al., 2007; Soba et al., 2007), Tutl does so only in the highly complex arbors of class IV neurons. We observed no genetic interactions between *Dscam* and *tutl* mutations, and have yet to find any evidence that Dscam and Tutl could act in a common molecular pathway to control dendrite self-avoidance. Future studies could reveal whether and how these seemingly distinct pathways converge but, based on our findings, we speculate that the molecular mechanisms ensuring dendrite self-avoidance will prove to be more complex than is appreciated currently.

Neither Tutl nor Dscam affect dendritic tiling among neurons of a similar functional type, illustrating that self-avoidance and tiling are likely to be mediated by distinct recognition molecules on the surfaces of dendrites.

How does Tutl regulate dendrite morphogenesis?

The full-length form of Tutl is a transmembrane protein with a five Ig/two FnIII ectodomain and a cytoplasmic tail, which suggests that it could act as a signaling receptor. Alternative splicing also gives rise to a membrane-tethered form that lacks the cytoplasmic tail (Bodily et al., 2001). This suggests that Tutl could also function as a membrane-bound ligand for an unknown receptor or, alternatively, as a co-receptor in a multiprotein receptor complex. These possibilities are not mutually exclusive, because Tutl could conceivably act as a ligand or a co-receptor in one cellular context, and as a signaling receptor in another. We found that the cytoplasmic tail was completely dispensable for the inhibition of dendrite branching in class I da neurons. This is consistent with a model in which Tutl acts as a ligand or a co-receptor in dendrites. By contrast, we found that the cytoplasmic tail was required to fully rescue viability in *tutl* mutants, suggesting that Tutl acts as a signaling receptor in this context.

It is currently unclear how Tutl controls dendrite branching and self-avoidance because our studies have not revealed a connection between Tutl and known regulators of dendrite morphogenesis such as Trc. We sought evidence for genetic interactions between *trc* and *tutl* and found none. These results alone cannot exclude the possibility that Trc and Tutl act in a common pathway to govern dendrite branching or self-avoidance, but it is noteworthy that the phenotypes of *trc* and *tutl* mutants also show some differences that could suggest they work through independent molecular pathways. Unlike *tutl*, *trc* is required for dendritic tiling among different class IV neurons, and *tutl* mutants do not display the excessive terminal branching in class IV neurons that is characteristic of *trc* mutants (Emoto et al., 2004).

The transcription factors Abrupt, Spineless, Knot and Cut each regulate patterns of dendrite branching in keeping with *tutl* mutations or Tutl overexpression (Crozatier and Vincent, 2008; Grueber et al., 2003; Hattori et al., 2007; Jinushi-Nakao et al., 2007; Kim et al., 2006; Li et al., 2004; Sugimura et al., 2004). However, in immunohistochemical studies of loss-of-function mutants for these transcription factors, we found it to be likely that Tutl expression is influenced by a regulatory program that is distinct from those involving Abrupt, Spineless, Knot or Cut.

Tutl remains somewhat enigmatic because we have yet to find evidence for a genetic or regulatory connection between *tutl* and genes with similar mutant phenotypes. Nevertheless, our discovery that Tutl regulates dendrite morphogenesis and the coverage of receptive territories underscores the fact that the molecular mechanisms that underlie dendrite morphogenesis remain incompletely understood. We can only speculate as to why *tutl* mutants have class-specific effects on dendrite morphogenesis, despite Tutl expression in all da neuron classes. Perhaps an unidentified Tutl-interacting protein, such as a receptor required for Tutl function, might be differentially expressed among da neurons and could thus account for the specificity of the phenotype. Other explanations may also exist. For example, it is possible that our MARCM experiments failed to show cell-autonomous defects in certain da neuron classes (classes II and III) because the requirement for Tutl in these cells was met by perdurance of sufficient Tutl protein inherited from the precursor cells of MARCM clones. Alternatively, Tutl in class II and class III da neurons might function non-cell autonomously to influence neighboring cell types.

Does Tutl promote dendrite branch repulsion?

It is intriguing that the two processes of branching and self-avoidance are related by a common requirement for *tutl*. Both phenotypes are consistent with the idea that Tutl promotes repulsion, perhaps between isoneuronal dendrite branches, or between dendrites and the substrata along which they grow. However, there is no direct evidence at this time for a repulsive role for Tutl. Simultaneous overexpression of Tutl in different da neuron classes was insufficient to induce branch repulsion among their dendrites. Together with our rescue experiments showing the dispensability of the cytoplasmic tail for dendrite branching, these data suggest that Tutl could function as a ligand or a co-receptor in complexes with one or more unidentified proteins at the cell surface. Such proteins might not be expressed in all da neurons, which could explain why *tutl* mutations do not affect da neuron classes II and III, and why Tutl cannot induce repulsion when overexpressed in overlapping neurons of Classes I-III. The *tutl* mutant phenotypes remain the strongest evidence of a repulsive role for Tutl, and it is likely that direct evidence for repulsion must await the identification of the relevant Tutl-interacting proteins.

If it is true that Tutl mediates repulsion, we speculate that the nature or degree of that repulsion could be influenced by the size of the dendritic arbor, leading to class-specific effects. Class I dendrites remain relatively small with Tutl protein distributed along the entire arbor, where Tutl-mediated repulsion could promote the collapse of transient interstitial branches that are known to extend during development (Gao et al., 1999) (branch inhibition). In large class IV arbors where Tutl is distributed more sparingly, Tutl-mediated repulsion could be one part of a multi-component system to redirect isoneuronal branches away from one another (self-avoidance) and thereby ensure proper distribution of dendrites over receptive territories (Hughes et al., 2007; Matthews et al., 2007; Soba et al., 2007). In this way, neurons of different classes could employ a common repulsive mechanism involving Tutl to sculpt arborization patterns of dramatically different complexity.

Is there an evolutionarily conserved role for Tutl-related proteins in dendrite morphogenesis in mammals?

Our findings that Tutl inhibits dendrite branching in *Drosophila* contrast with initial observations in cultured rodent neurons, in which RNAi-knockdown experiments suggested that the Tutl ortholog Dasm1 was required to promote dendritic outgrowth (Shi et al., 2004). However, it was recently argued that these RNAi findings were due to off-target effects (Mishra et al., 2008). The role of Dasm1 in mammalian dendrite morphogenesis is currently unclear, as *Dasm1* knockout mice have no observable dendritic defects (Mishra et al., 2008). However, the possibility has been raised that Dasm1 function in dendrites is redundant with the function of Igsf9b, a closely related protein that is coexpressed in the developing hippocampus, the expression of which is unaltered in the brains of *Dasm1* knockout mice (Mishra et al., 2008). Loss-of function studies for both Dasm1 and Igsf9b should reveal whether Tutl-like proteins in mammals share with Tutl an evolutionarily conserved role in dendrite morphogenesis.

Acknowledgements

We thank Fen-Biao Gao, Wayne Johnson, Liqun Luo, Yuh Nung Jan, Bing Ye, Susan Younger, Dietmar Schmucker, Adrian Moore, the Bloomington and Harvard stock centers, and the *Drosophila* Genomic Resource Centre for fly stocks and reagents. We also thank Michael Haber for help in quantifying dendrite parameters, and Keith Murai, Matthias Landgraf, Catriona McDonald and members of the Rao and van Meyel laboratories for advice. The work was supported by funds from the Canadian Institutes of Health Research (CIHR Team Grant to Y.R. and D.J.v.M., Operating Grant to Y.R., International Opportunities Grant to D.J.v.M.), the Research Institute of the McGill University Health Centre (D.J.v.M.), and the Canadian Foundation for Innovation. Y.R. is an FRSQ Senior Research Scholar. D.J.v.M. is a CIHR New Investigator.

Supplementary material

Supplementary material for this article is available at http://dev.biologists.org/cgi/content/full/136/20/3475/DC1

References

Bodily, K. D., Morrison, C. M., Renden, R. B. and Broadie, K. (2001). A novel member of the Ig superfamily, turtle, is a CNS-specific protein required for coordinated motor control. *J. Neurosci.* **21**, 3113-3125.

Campbell, D. S., Stringham, S. A., Timm, A., Xiao, T., Law, M. Y., Baier, H., Nonet, M. L. and Chien, C. B. (2007). Slit1a inhibits retinal ganglion cell arborization and synaptogenesis via Robo2-dependent and -independent pathways. *Neuron* **55**, 231-245.

Crozatier, M. and Vincent, A. (2008). Control of multidendritic neuron differentiation in Drosophila: the role of Collier. *Dev. Biol.* **315**, 232-242.

Dimitrova, S., Reissaus, A. and Tavosanis, G. (2008). Slit and Robo regulate dendrite branching and elongation of space-filling neurons in Drosophila. *Dev. Biol.* **324**, 18-30.

Doudney, K., Murdoch, J. N., Braybrook, C., Paternotte, C., Bentley, L., Copp, A. J. and Stanier, P. (2002). Cloning and characterization of Igsf9 in mouse and human: a new member of the immunoglobulin superfamily expressed in the developing nervous system. *Genomics* **79**, 663-670.

Emoto, K., He, Y., Ye, B., Grueber, W. B., Adler, P. N., Jan, L. Y. and Jan, Y. N. (2004). Control of dendritic branching and tiling by the Tricornered-kinase/Furry signaling pathway in Drosophila sensory neurons. *Cell* **119**, 245-256.

Fiala, J. C. (2005). Reconstruct: a free editor for serial section microscopy. *J. Microsc.* **218**, 52-61.

Fuerst, P. G., Koizumi, A., Masland, R. H. and Burgess, R. W. (2008). Neurite arborization and mosaic spacing in the mouse retina require DSCAM. *Nature* **451**, 470-474.

Furrer, M. P., Kim, S., Wolf, B. and Chiba, A. (2003). Robo and Frazzled/DCC mediate dendritic guidance at the CNS midline. *Nat. Neurosci.* **6**, 223-230.

Furrer, M. P., Vasenkova, I., Kamiyama, D., Rosado, Y. and Chiba, A. (2007). Slit and Robo control the development of dendrites in Drosophila CNS. *Development* **134**, 3795-3804.

Gao, F. B., Brenman, J. E., Jan, L. Y. and Jan, Y. N. (1999). Genes regulating dendritic outgrowth, branching, and routing in Drosophila. *Genes Dev.* **13**, 2549-2561.

Gao, F. B., Kohwi, M., Brenman, J. E., Jan, L. Y. and Jan, Y. N. (2000). Control of dendritic field formation in Drosophila: the roles of flamingo and competition between homologous neurons. *Neuron* **28**, 91-101.

Godenschwege, T. A., Simpson, J. H., Shan, X., Bashaw, G. J., Goodman, C. S. and Murphey, R. K. (2002). Ectopic expression in the giant fiber system of Drosophila reveals distinct roles for roundabout (Robo), Robo2, and Robo3 in dendritic guidance and synaptic connectivity. *J. Neurosci.* **22**, 3117-3129.

Grueber, W. B., Jan, L. Y. and Jan, Y. N. (2002). Tiling of the Drosophila epidermis by multidendritic sensory neurons. *Development* **129**, 2867-2878.

Grueber, W. B., Jan, L. Y. and Jan, Y. N. (2003). Different levels of the homeodomain protein cut regulate distinct dendrite branching patterns of Drosophila multidendritic neurons. *Cell* **112**, 805-818.

Hattori, Y., Sugimura, K. and Uemura, T. (2007). Selective expression of Knot/Collier, a transcriptional regulator of the EBF/Olf-1 family, endows the Drosophila sensory system with neuronal class-specific elaborated dendritic patterns. *Genes Cells* **12**, 1011-1022.

Horch, H. W. and Katz, L. C. (2002). BDNF release from single cells elicits local dendritic growth in nearby neurons. *Nat. Neurosci.* **5**, 1177-1184.

Hughes, M. E., Bortnick, R., Tsubouchi, A., Baumer, P., Kondo, M., Uemura, T. and Schmucker, D. (2007). Homophilic Dscam interactions control complex dendrite morphogenesis. *Neuron* **54**, 417-427.

Hummel, T., Vasconcelos, M. L., Clemens, J. C., Fishilevich, Y., Vosshall, L. B. and Zipursky, S. L. (2003). Axonal targeting of olfactory receptor neurons in Drosophila is controlled by Dscam. *Neuron* **37**, 221-231.

Jinushi-Nakao, S., Arvind, R., Amikura, R., Kinameri, E., Liu, A. W. and Moore, A. W. (2007). Knot/Collier and cut control different aspects of dendrite cytoskeleton and synergize to define final arbor shape. *Neuron* **56**, 963-978.

Kim, M. D., Jan, L. Y. and Jan, Y. N. (2006). The bHLH-PAS protein Spineless is necessary for the diversification of dendrite morphology of Drosophila dendritic arborization neurons. *Genes Dev.* **20**, 2806-2819.
Kimura, H., Usui, T., Tsubouchi, A. and Uemura, T. (2006). Potential dual molecular interaction of the Drosophila 7-pass transmembrane cadherin Flamingo in dendritic morphogenesis. *J. Cell Sci.* **119**, 1118-1129.
Komiyama, T., Sweeney, L. B., Schuldiner, O., Garcia, K. C. and Luo, L. (2007). Graded expression of semaphorin-1a cell-autonomously directs dendritic targeting of olfactory projection neurons. *Cell* **128**, 399-410.
Lee, T. and Luo, L. (1999). Mosaic analysis with a repressible cell marker for studies of gene function in neuronal morphogenesis. *Neuron* **22**, 451-461.
Li, W., Wang, F., Menut, L. and Gao, F. B. (2004). BTB/POZ-zinc finger protein abrupt suppresses dendritic branching in a neuronal subtype-specific and dosage-dependent manner. *Neuron* **43**, 823-834.
Matthews, B. J., Kim, M. E., Flanagan, J. J., Hattori, D., Clemens, J. C., Zipursky, S. L. and Grueber, W. B. (2007). Dendrite self-avoidance is controlled by Dscam. *Cell* **129**, 593-604.
Mishra, A., Knerr, B., Paixao, S., Kramer, E. R. and Klein, R. (2008). Dendrite arborization and synapse maturation (Dasm)-1 is dispensable for dendrite arborization. *Mol. Cell. Biol.* **28**, 2782-2791.
Ou, Y., Chwalla, B., Landgraf, M. and van Meyel, D. J. (2008). Identification of genes influencing dendrite morphogenesis in developing peripheral sensory and central motor neurons. *Neural Dev.* **3**, 16.
Parks, A. L., Cook, K. R., Belvin, M., Dompe, N. A., Fawcett, R., Huppert, K., Tan, L. R., Winter, C. G., Bogart, K. P., Deal, J. E. et al. (2004). Systematic generation of high-resolution deletion coverage of the Drosophila melanogaster genome. *Nat. Genet.* **36**, 288-292.
Parrish, J. Z., Emoto, K., Kim, M. D. and Jan, Y. N. (2007). Mechanisms that regulate establishment, maintenance, and remodeling of dendritic fields. *Annu. Rev. Neurosci.* **30**, 399-423.
Polleux, F., Morrow, T. and Ghosh, A. (2000). Semaphorin 3A is a chemoattractant for cortical apical dendrites. *Nature* **404**, 567-573.
Schmitt, A. M., Shi, J., Wolf, A. M., Lu, C. C., King, L. A. and Zou, Y. (2006). Wnt-Ryk signalling mediates medial-lateral retinotectal topographic mapping. *Nature* **439**, 31-37.
Shi, S. H., Cox, D. N., Wang, D., Jan, L. Y. and Jan, Y. N. (2004). Control of dendrite arborization by an Ig family member, dendrite arborization and synapse maturation 1 (Dasm1). *Proc. Natl. Acad. Sci. USA* **101**, 13341-13345.
Shima, Y., Kawaguchi, S. Y., Kosaka, K., Nakayama, M., Hoshino, M., Nabeshima, Y., Hirano, T. and Uemura, T. (2007). Opposing roles in neurite growth control by two seven-pass transmembrane cadherins. *Nat. Neurosci.* **10**, 963-969.
Soba, P., Zhu, S., Emoto, K., Younger, S., Yang, S. J., Yu, H. H., Lee, T., Jan, L. Y. and Jan, Y. N. (2007). Drosophila sensory neurons require Dscam for dendritic self-avoidance and proper dendritic field organization. *Neuron* **54**, 403-416.
Sugimura, K., Satoh, D., Estes, P., Crews, S. and Uemura, T. (2004). Development of morphological diversity of dendrites in Drosophila by the BTB-zinc finger protein abrupt. *Neuron* **43**, 809-822.
Sweeney, N. T., Li, W. and Gao, F. B. (2002). Genetic manipulation of single neurons in vivo reveals specific roles of flamingo in neuronal morphogenesis. *Dev. Biol.* **247**, 76-88.
Whitford, K. L., Marillat, V., Stein, E., Goodman, C. S., Tessier-Lavigne, M., Chedotal, A. and Ghosh, A. (2002). Regulation of cortical dendrite development by Slit-Robo interactions. *Neuron* **33**, 47-61.
Yamamoto, M., Ueda, R., Takahashi, K., Saigo, K. and Uemura, T. (2006). Control of axonal sprouting and dendrite branching by the Nrg-Ank complex at the neuron-glia interface. *Curr. Biol.* **16**, 1678-1683.
Yates, P. A., Roskies, A. L., McLaughlin, T. and O'Leary, D. D. (2001). Topographic-specific axon branching controlled by ephrin-As is the critical event in retinotectal map development. *J. Neurosci.* **21**, 8548-8563.